Anionic, Four-co-ordinate, Ten-electron Bismuth Complexes: Aspects of Synthesis, Structure and Bonding†

William Clegg,[a] Neville A. Compton,[a] R. John Errington,[a] George A. Fisher,[a] David C. R. Hockless,[a] Nicholas C. Norman,*[,a] A. Guy Orpen*[,b] and Susan E. Stratford[b]

[a] *Department of Chemistry, The University of Newcastle, Newcastle upon Tyne NE1 7RU, UK*

[b] *Department of Chemistry, The University, Bristol BS8 1TS, UK*

The reaction between $[BiCl\{Fe(CO)_2(\eta\text{-}C_5H_5)\}_2]$ **1** and 1 equivalent of $[N(PPh_3)_2]Cl$ afforded the ionic complex $[N(PPh_3)_2][BiCl_2\{Fe(CO)_2(\eta\text{-}C_5H_5)\}_2]$ **2**. The $[NMe_4]^+$ salt, $[NMe_4][BiCl_2\{Fe(CO)_2(\eta\text{-}C_5H_5)\}_2]$ **3**, was prepared similarly. An analogous bromide derivative, $[PPh_4][BiBr_2\{Fe(CO)_2(\eta\text{-}C_5H_5)\}_2]$ **4**, was prepared from the reaction between $[BiBr\{Fe(CO)_2(\eta\text{-}C_5H_5)\}_2]$ **5** and $[PPh_4]Br$. The reaction between $[BiCl\{Mo(CO)_3(\eta\text{-}C_5H_5)\}_2]$ **7** and 1 equivalent of $[N(PPh_3)_2]Cl$ afforded the complex $[N(PPh_3)_2][BiCl_2\{Mo(CO)_3(\eta\text{-}C_5H_5)\}_2]$ **8**; that between $[PPh_3(CH_2Ph)]Cl$ and **7** afforded $[PPh_3(CH_2Ph)][BiCl_2\{Mo(CO)_3(\eta\text{-}C_5H_5)\}_2]$ **9**. In tetrahydrofuran (thf) solution some degree of dissociation of $[Mo(CO)_3(\eta\text{-}C_5H_5)]^-$ is observed for **8** and **9**. The bromide complexes $[PPh_4][BiBr_2\{Mo(CO)_3(\eta\text{-}C_5H_5)\}_2]$ **10** and $[NBu^n_4][BiBr_2\{Mo(CO)_3(\eta\text{-}C_5H_5)\}_2]$ **11** were prepared from the reactions between $[BiBr\{Mo(CO)_3(\eta\text{-}C_5H_5)\}_2]$ **12** and 1 equivalent of $[PPh_4]Br$ and $[NBu^n_4]Br$ respectively. The tungsten complexes $[N(PPh_3)_2][BiCl_2\{W(CO)_3(\eta\text{-}C_5H_5)\}_2]$ **13** and $[PPh_3(CH_2Ph)][BiCl_2\{W(CO)_3(\eta\text{-}C_5H_5)\}_2]$ **14** were similarly prepared. Spectroscopic data for the complexes $[N(PPh_3)_2][BiCl_3\{Mo(CO)_3(\eta\text{-}C_5H_5)\}]$ **16** and $[N(PPh_3)_2][BiCl_3\{W(CO)_3(\eta\text{-}C_5H_5)\}]$ **17** are also presented. The structures of compounds **2**, **8**, **9** (as a thf solvate) and **13** were determined by X-ray crystallography. The structures of all of the compounds comprise a four-co-ordinate bismuth centre bonded to two chlorine atoms and two ML_n fragments. The precise co-ordination geometries, however, vary from close to an idealised equatorially-vacant trigonal bipyramid (disphenoidal), **2** and **9**, with axial chlorines and equatorial metal centres, to nearly tetrahedral, **8** and **13**. These results are incorporated into a general discussion of the structures found for AB_4E complexes, *i.e.* four-co-ordinate with ten valence electrons, and some ideas are advanced on possible electronic factors which determine the particular geometry adopted.

In a series of papers, we have described the syntheses of a range of compounds of the general formula $[BiX(ML_n)_2]$ where X is halide and ML_n is a 17-electron organotransition-metal fragment, such as $Mo(CO)_3(\eta\text{-}C_5H_5)$, $Fe(CO)_2(\eta\text{-}C_5H_5)$ or $Mn(CO)_5$.[1–6] We were particularly interested in the structures of these molecules and noted that, in almost all cases, the appreciable Lewis acidity of the bismuth centre resulted in oligomerisation, in the solid state, through intermolecular X–Bi···X interactions with a concomitant increase in the co-ordination number of the bismuth to four. As an extension of this work, and exploiting further the Lewis acidity of the bismuth centre, we recently reported preliminary details of the reactions between $[BiX(ML_n)_2]$ and X^- which afforded the monomeric, anionic complexes $[BiX_2(ML_n)_2]^-$.[7] Herein, we provide a full account of this study and comment on the structures of these and related compounds.

Results and Discussion

Syntheses and Spectroscopic Characterisation.—Treatment of a tetrahydrofuran (thf) solution of $[BiCl\{Fe(CO)_2(\eta\text{-}C_5H_5)\}_2]$ **1**[1,8] with 1 equivalent of $[N(PPh_3)_2]Cl$ afforded, after work-up, dark green crystals of the ionic complex $[N(PPh_3)_2][BiCl_2\{Fe(CO)_2(\eta\text{-}C_5H_5)\}_2]$ **2**. Spectroscopic and analytical data for **2**, and all new complexes, are given in Table 1 and were consistent with the proposed formula; a solution infrared spectrum (thf) of **2** is shown in Fig. 1(*a*). The $[NMe_4]^+$ salt $[NMe_4][BiCl_2\{Fe(CO)_2(\eta\text{-}C_5H_5)\}_2]$ **3** was prepared similarly. An analogous bromide derivative, $[PPh_4][BiBr_2\{Fe(CO)_2(\eta\text{-}C_5H_5)\}_2]$ **4**, was prepared from the reaction between $[BiBr\{Fe(CO)_2(\eta\text{-}C_5H_5)\}_2]$ **5** and $[PPh_4]Br$. Complex **5** has been previously described by Schmidbaur and co-workers[8] who reported infrared data in CH_2Cl_2 solution; data in thf solution are given in Table 1 and the spectrum is shown for comparison in Fig. 1(*b*).‡ We also tried to make the iodide derivatives from

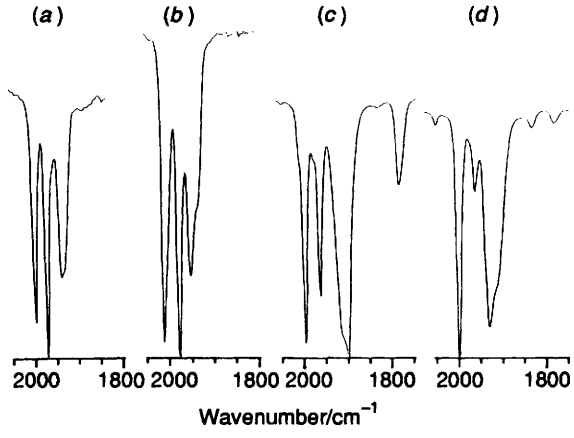

Fig. 1 Infrared spectra in thf solution in the carbonyl stretching region for complexes **2**(*a*), **5**(*b*), **8**(*c*) and **16**(*d*)

† *Supplementary data available:* see Instructions for Authors, *J. Chem. Soc., Dalton Trans.*, 1992, Issue 1, pp. xx–xxv.

‡ Comparison of the spectra in thf solution for the complexes $[BiX\{Fe(CO)_2(\eta\text{-}C_5H_5)\}_2]$[1] and $[BiX_2\{Fe(CO)_2(\eta\text{-}C_5H_5)\}_2]^-$ [*i.e.* Fig. 1(*b*) *vs.* Fig. 1(*a*)] reveal that their appearance is very similar, the only difference being a shift to lower frequency of about 5–8 cm^{-1} for the anionic complexes.

Table 1 Spectroscopic and analytical data for the complexes

Compound	ν(CO)[a]/cm^{-1}	Analysis[b] (%) C	H	N
2 $[N(PPh_3)_2][BiCl_2\{Fe(CO)_2(\eta\text{-}C_5H_5)\}_2]$	1998m, 1974s, 1937m	50.60 (51.20)	3.25 (3.40)	1.10 (1.20)
3 $[NMe_4][BiCl_2\{Fe(CO)_2(\eta\text{-}C_5H_5)\}_2]$	2011m, 1978s, 1952m			
4 $[PPh_4][BiBr_2\{Fe(CO)_2(\eta\text{-}C_5H_5)\}_2]$	2004s, 1972s, 1943m			
5 $[BiBr\{Fe(CO)_2(\eta\text{-}C_5H_5)\}_2]$	2012s, 1977s, 1952m[c]			
6 $[BiI\{Fe(CO)_2(\eta\text{-}C_5H_5)\}_2]$	2011s, 1979s, 1953m			
8 $[N(PPh_3)_2][BiCl_2\{Mo(CO)_3(\eta\text{-}C_5H_5)\}_2]$	2052w, 1996s, 1962m, 1899br s, 1781m	47.20 (47.70)	2.85 (3.10)	1.05 (1.05)
9 $[PPh_3(CH_2Ph)][BiCl_2\{Mo(CO)_3(\eta\text{-}C_5H_5)\}_2]$	1998s, 1965m, 1905br s, 1783w	45.10 (43.80)	3.25 (2.85)	
10 $[PPh_4][BiBr_2\{Mo(CO)_3(\eta\text{-}C_5H_5)\}_2]$	2046w, 1996s, 1962s, 1904br s, 1839w, 1783w	39.95 (40.10)	2.45 (2.50)	
11 $[NBu^n_4][BiBr_2\{Mo(CO)_3(\eta\text{-}C_5H_5)\}_2]$	1996s, 1962m, 1907br s			
13 $[N(PPh_3)_2][BiCl_2\{W(CO)_3(\eta\text{-}C_5H_5)\}_2]$	1991s, 1958s, 1895br s, 1777w	41.95 (42.05)	2.60 (2.70)	0.95 (0.95)
14 $[PPh_3(CH_2Ph)][BiCl_2\{W(CO)_3(\eta\text{-}C_5H_5)\}_2]$	2006s, 1960s, 1899br s, 1817w			
16 $[N(PPh_3)_2][BiCl_3\{Mo(CO)_3(\eta\text{-}C_5H_5)\}]$	2053w, 2000s, 1962m, 1929br s, 1831w, 1781w			
17 $[N(PPh_3)_2][BiCl_3\{W(CO)_3(\eta\text{-}C_5H_5)\}]$	1995s, 1958m, 1922s, 1900s, 1809m, 1777w			

[a] Measured in thf solution. [b] Calculated values in parentheses. [c] The values for **5** in CH_2Cl_2 given in ref. 8 are 2009s, 1984s, 1957s, 1934s (sh).

reactions between $[BiI\{Fe(CO)_2(\eta\text{-}C_5H_5)\}_2]$ **6** and sources of iodide but these reactions were unsuccessful. Data for **6** are presented in Table 1 since this complex has not been previously described and details of the synthesis are given in the Experimental section. As with the molybdenum analogue,[5] we found that the best route to the iodide was from the trimetal complex $[Bi\{Fe(CO)_2(\eta\text{-}C_5H_5)\}_3]$[1,8] and I_2 rather than using BiI_3 and 2 equivalents of $K[Fe(CO)_2(\eta\text{-}C_5H_5)]$.

The reaction between $[BiCl\{Mo(CO)_3(\eta\text{-}C_5H_5)\}_2]$ **7**[2] and 1 equivalent of $[N(PPh_3)_2]Cl$ afforded the complex $[N(PPh_3)_2][BiCl_2\{Mo(CO)_3(\eta\text{-}C_5H_5)\}_2]$ **8** whilst the reaction between $[PPh_3(CH_2Ph)]Cl$ and **7** afforded $[PPh_3(CH_2Ph)][BiCl_2\{Mo(CO)_3(\eta\text{-}C_5H_5)\}_2]$ **9**. Spectroscopic data for both complexes are given in Table 1 and the infrared spectrum of **8** in thf is shown in Fig. 1(*c*). The overall pattern of the carbonyl absorptions in **8** is characteristic of a $Bi\{Mo(CO)_3(\eta\text{-}C_5H_5)\}_2$ fragment [see Fig. 5(*c*) in ref. 2] but the absorption at 1781 cm^{-1} is due to the presence of $[Mo(CO)_3(\eta\text{-}C_5H_5)]^-$ and is therefore indicative of some degree of dissociation in thf solution; a similar situation is seen for **9** although it is noteworthy that the spectra are slightly different suggestive of a degree of ion pairing. We have not previously observed dissociation behaviour for any of the neutral bismuth transition–metal complexes[1–5] in solution but this phenomenon is commonly found for the analogous indium transition–metal complexes.[9–11] This reflects a larger degree of ionic character for In^{III} *vs.* Bi^{III}, an expected trend for these two elements in view of the higher electronegativity of bismuth, but it is not surprising that dissociation behaviour is observed for bismuth complexes when an overall negative charge is present. The bromide complexes $[PPh_4][BiBr_2\{Mo(CO)_3(\eta\text{-}C_5H_5)\}_2]$ **10** and $[NBu^n_4][BiBr_2\{Mo(CO)_3(\eta\text{-}C_5H_5)\}_2]$ **11** were prepared from the reactions between $[BiBr\{Mo(CO)_3(\eta\text{-}C_5H_5)\}_2]$ **12**[5] and 1 equivalent of $[PPh_4]Br$ and $[NBu^n_4]Br$ respectively data for which are given in Table 1.

The tungsten complexes $[N(PPh_3)_2][BiCl_2\{W(CO)_3(\eta\text{-}C_5H_5)\}_2]$ **13** and $[PPh_3(CH_2Ph)][BiCl_2\{W(CO)_3(\eta\text{-}C_5H_5)\}_2]$ **14** were prepared from the reaction between $[BiCl\{W(CO)_3(\eta\text{-}C_5H_5)\}_2]$ **15**[2] and 1 equivalent of $[N(PPh_3)_2]Cl$ and $[PPh_3(CH_2Ph)]Cl$ respectively. Infrared data (Table 1) indicated that these compounds were similar in all respects to the molybdenum analogues including the small degree of dissociation evident in thf solution.

We also carried out reactions between $[N(PPh_3)_2]Cl$ and both the cobalt complex $[BiCl\{Co(CO)_3(PPh_3)\}_2]$[3] and the manganese complex $[BiCl\{Mn(CO)_5\}_2]$.[4] The former reaction showed no evidence for a dichloro anionic complex analogous to those described above but gave only $[BiCl_2\{Co(CO)_3(PPh_3)\}]$[3] and $[Co(CO)_4]^-$ as judged by infrared spectroscopy. The reactions involving the manganese complex led only to decomposition.

Table 2 Selected bond lengths (Å) and angles (°) for the complexes **2**, **8**, **9**·thf and **13**

Compound				
2	Bi–Cl(1)	2.773(6)	Cl(1)–Bi–Cl(2)	155.6(2)
	Bi–Cl(2)	2.818(8)	Cl(1)–Bi–Fe(1)	98.4(2)
	Bi–Fe(1)	2.679(3)	Cl(2)–Bi–Fe(1)	95.6(2)
	Bi–Fe(2)	2.679(3)	Cl(1)–Bi–Fe(2)	94.1(2)
			Cl(2)–Bi–Fe(2)	99.4(2)
			Fe(1)–Bi–Fe(2)	111.4(1)
8	Bi–Cl(1)	2.709(6)	Cl(1)–Bi–Cl(2)	138.5(1)
	Bi–Cl(2)	2.850(4)	Cl(1)–Bi–Mo(1)	95.6(2)
	Bi–Mo(1)	2.944(1)	Cl(2)–Bi–Mo(1)	96.3(1)
	Bi–Mo(2)	3.032(2)	Cl(1)–Bi–Mo(2)	104.0(1)
			Cl(2)–Bi–Mo(2)	105.8(1)
			Mo(1)–Bi–Mo(2)	116.4(1)
9	Bi–Cl(1)	2.724(3)	Cl(1)–Bi–Cl(2)	154.7(1)
	Bi–Cl(2)	2.907(2)	Cl(1)–Bi–Mo(1)	92.1(1)
	Bi–Mo(1)	3.023(1)	Cl(2)–Bi–Mo(1)	106.1(1)
	Bi–Mo(2)	2.978(1)	Cl(1)–Bi–Mo(2)	96.9(1)
			Cl(2)–Bi–Mo(2)	90.4(1)
			Mo(1)–Bi–Mo(2)	117.0(1)
13	Bi–Cl(1)	2.714(6)	Cl(1)–Bi–Cl(2)	139.8(2)
	Bi–Cl(2)	2.877(5)	Cl(1)–Bi–W(1)	104.4(1)
	Bi–W(1)	3.029(1)	Cl(2)–Bi–W(1)	105.5(1)
	Bi–W(2)	2.943(1)	Cl(1)–Bi–W(2)	94.7(2)
			Cl(2)–Bi–W(2)	95.6(1)
			W(1)–Bi–W(2)	116.2(1)

Finally in this section, we mention some reactions designed to give complexes of the general formula $[BiCl_3(ML_n)]^-$. The reaction between $[BiCl_2\{Mo(CO)_3(\eta\text{-}C_5H_5)\}]$[2] and $[N(PPh_3)_2]Cl$ afforded a copper-coloured product, the infrared spectrum of which is shown in Fig. 1(*d*). An identical spectrum was obtained for the product of the reaction between **8** and $[N(PPh_3)_2][BiCl_4]$ and we propose that this complex is most probably the desired species $[N(PPh_3)_2][BiCl_3\{Mo(CO)_3(\eta\text{-}C_5H_5)\}]$ **16** although we were not able to obtain satisfactory analytical data on this material. It is again evident from the infrared spectrum that a small degree of dissociation occurs in thf solution which, on the basis of what we said above, can be taken as evidence of an anionic complex. The reaction between **13** and $[N(PPh_3)_2][BiCl_4]$ afforded a similar complex formulated as $[N(PPh_3)_2][BiCl_3\{W(CO)_3(\eta\text{-}C_5H_5)\}]$ **17**.

Structural Characterisation.—The structures of compounds **2**, **8**, **9** (as a thf solvate) and **13** were determined by X-ray crystallography and the results are shown in Figs. 2, 3, 4 and 5 respectively. Selected bond lengths and angles for all structures

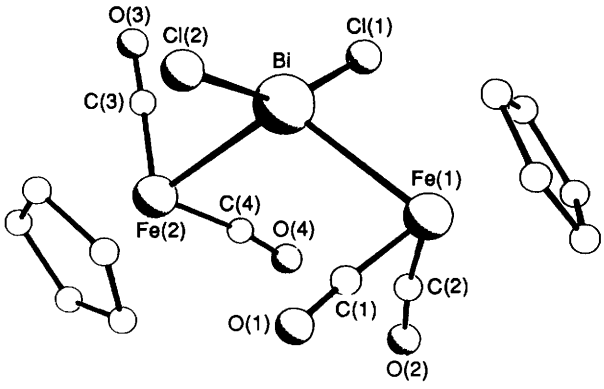

Fig. 2 A view of the $[BiCl_2\{Fe(CO)_2(\eta\text{-}C_5H_5)\}_2]^-$ anion of **2** showing the atom numbering scheme. Hydrogen atoms omitted for clarity

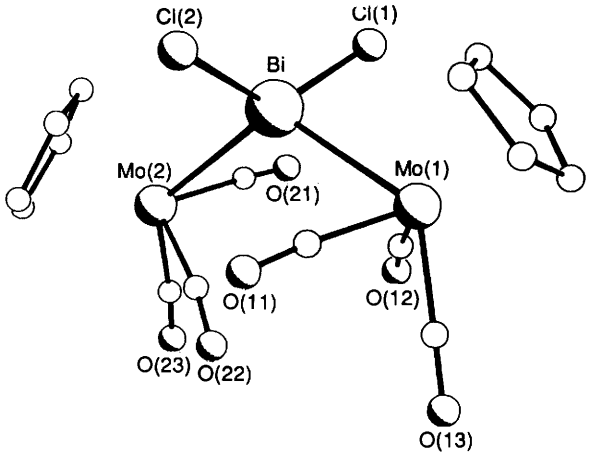

Fig. 3 A view of the $[BiCl_2\{Mo(CO)_3(\eta\text{-}C_5H_5)\}_2]^-$ anion of **8** showing the atom numbering scheme. Hydrogen atoms omitted for clarity

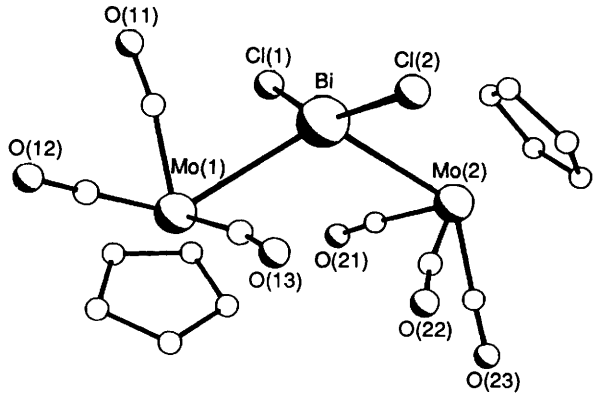

Fig. 4 A view of the $[BiCl_2\{Mo(CO)_3(\eta\text{-}C_5H_5)\}_2]^-$ anion of **9** showing the atom numbering scheme. Hydrogen atoms omitted for clarity

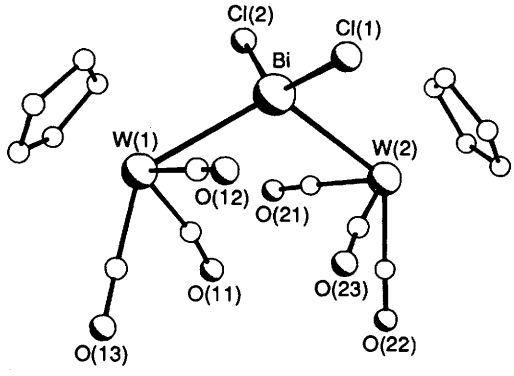

Fig. 5 A view of the $[BiCl_2\{W(CO)_3(\eta\text{-}C_5H_5)\}_2]^-$ anion of **13** showing the atom numbering scheme. Hydrogen atoms omitted for clarity

are given in Table 2, atomic positional parameters are presented in Tables 3–6 and crystallographic data are collected in Table 7. Compounds **8** and **13** are isomorphous.

The structures of all of the compounds comprise a four-co-ordinate bismuth centre bonded to two chlorine atoms and two ML_n fragments. The Bi–Cl distances are in the range 2.7–2.9 Å and are thus somewhat longer than a standard Bi–Cl single-bond length as found, for example, in the monomeric complex $[BiCl\{Mo(CO)_2(CNBu^t)(\eta\text{-}C_5H_5)\}_2][Bi\text{–}Cl\ 2.610(2)\ Å]$[2] but are within the range found for Bi–Cl bonds when intermolecular Cl–Bi · · · Cl bonding is present.[1,2,4,5] The Bi–M bond lengths are also within, or close to, normal ranges. For complex **2** the Bi–Fe distances are similar to those observed in other related bismuth–iron complexes[1,8,12] whilst the Bi–Mo and Bi–W bond lengths are only slightly longer (approximately 0.1 Å) than those found in complexes such as **7**, **12** and **15**.[2,5]

Of more interest are the interbond angles in these compounds and we will concentrate on two, the M–Bi–M and Cl–Bi–Cl angles (α and β respectively). The former for **2** is 111.4(1)° whilst those for **8**, **9** and **13** range from 116.2(1)–117.0(1)°. The latter angles, however, show a much larger range; for **2** and **9** the angles are 155.6(2) and 154.7(1)° respectively whereas for **8** and **13** they are 138.5(1) and 139.8(2)°. The large difference between **8** and **9** is noteworthy and presumably results from the effect of different cations and the presence of one thf molecule per ion pair in crystals of **9**. If we consider the structures of **2** and **9**, it is clear that the co-ordination geometry around the bismuth centre can reasonably be described as equatorially-vacant trigonal bipyramidal, or disphenoidal, with the metal atoms in equatorial sites and *trans*, axial chlorines. This structure is largely that expected from valence shell electron pair repulsion (VSEPR) arguments[13] for a four-co-ordinate centre with ten valence electrons (five pairs and AB_4E in Gillespie's terminology)[13] and as such we would presume that the non-bonding electron pair occupies the remaining equatorial site. Moreover, assuming that chlorine is more electronegative than either of the metal fragments, we would also expect these atoms to reside in the axial positions in line with this well known site preference for electronegative elements or groups in trigonal-bipyramidal molecules (see below).[14] With this in mind, it is apparent that the structures of **8** and **13** cannot be satisfactorily described by this geometry since the Cl–Bi–Cl angles are more than 40° from an idealised value of 180°. They are in fact closer to the tetrahedral angle which implies that a description (albeit rather imprecise) of distorted tetrahedral is more appropriate than disphenoidal. We proposed a possible electronic origin for this distortion in ref. 7 and will return to this matter in more detail later, but at this point it will be useful to look at the structures of AB_4E molecules in general in order to place this discussion in a proper perspective.

As mentioned above, the most common AB_4E structure is disphenoidal. This is exemplified by SF_4 and shown diagramatically in **A**. The interbond angle in the equatorial plane is often much less than 120° whilst the angle between the axial groups is usually a little less than 180° with the axial B groups displaced *towards* the equatorial B groups. Moreover, there is quite a range of angles observed as illustrated by two examples from bismuth chemistry, namely $Rb[Bi(SCN)_4]$ (α = 92.6, β = 158.2°)[15] and $[BiPh_4][Bi\{OC(O)CF_3\}_2Ph_2]$ (α = 95, β = 172°).[16] Two further examples, from solid-state bismuth chemistry, are found in the structures of $\beta\text{-}Bi_2O_3$ (α = 82.4, β = 172.1°)[17] and $BaBiO_{2.5}$ (α = 91.5, β = 171.4°),[18] the former having an inter-equatorial bond angle significantly less than 90°! The relationships between these two bond angles and

Table 3 Atomic coordinates for complex **2**

Atom	*x*	*y*	*z*	Atom	*x*	*y*	*z*
Bi	0.139 20(8)	0.142 62(2)	0.036 01(5)	C(122)	1.064(1)	0.197 6(4)	0.585 0(7)
Cl(1)	0.083 0(8)	0.127 0(2)	0.215 4(4)	C(123)	1.216	0.204 6	0.579 6
Cl(2)	0.268 5(7)	0.182 2(2)	−0.107 4(5)	C(124)	1.286	0.199 6	0.497 9
Fe(1)	−0.141 9(3)	0.151 71(7)	−0.024 8(2)	C(125)	1.204	0.187 4	0.421 5
C(1)	−0.092(2)	0.144 0(9)	−0.133(1)	C(126)	1.053	0.180 3	0.426 8
O(1)	−0.063(2)	0.139 0(8)	−0.207(1)	C(121)	0.982	0.185 4	0.508 6
C(2)	−0.197(2)	0.104 6(7)	−0.008(2)	C(132)	0.617(1)	0.178 2(3)	0.663 6(8)
O(2)	−0.240(2)	0.073 3(6)	−0.005(1)	C(133)	0.545	0.199 2	0.728 9
C(11)	−0.119(3)	0.209 6(7)	0.015(2)	C(134)	0.568	0.238 5	0.736 0
C(12)	−0.162(3)	0.187 3(8)	0.086(2)	C(135)	0.664	0.256 7	0.677 9
C(13)	−0.305(4)	0.172(1)	0.063(2)	C(136)	0.737	0.235 7	0.612 6
C(14)	−0.344(3)	0.183 9(9)	−0.026(3)	C(131)	0.714	0.196 4	0.605 5
C(15)	−0.227(4)	0.204 8(7)	−0.057(2)	P(2)	0.864 9(4)	0.086 0(1)	0.532 0(3)
Fe(2)	0.238 8(3)	0.072 21(8)	0.002 0(2)	C(212)	0.810(1)	0.076 3(3)	0.351 0(9)
C(3)	0.356(3)	0.079 6(6)	0.097(2)	C(213)	0.746	0.058 7	0.274 7
O(3)	0.434(2)	0.083 3(6)	0.160(2)	C(214)	0.663	0.025 3	0.284 0
C(4)	0.097(3)	0.053 5(6)	0.060(1)	C(215)	0.645	0.009 6	0.369 5
O(4)	−0.001(2)	0.039 2(5)	0.098(1)	C(216)	0.709	0.027 2	0.445 8
C(21)	0.243(3)	0.085 4(8)	−0.135(1)	C(211)	0.792	0.060 6	0.436 5
C(22)	0.165(3)	0.051 5(8)	−0.125(2)	C(222)	0.910(1)	0.024 5(3)	0.644 4(8)
C(23)	0.273(3)	0.027 7(6)	−0.082(2)	C(223)	0.875	0.000 6	0.716 0
C(24)	0.405(3)	0.044 5(7)	−0.070(2)	C(224)	0.759	0.009 9	0.771 9
C(25)	0.386(2)	0.082 4(6)	−0.098(2)	C(225)	0.677	0.043 2	0.756 2
N	0.779(1)	0.124 5(4)	0.543 0(8)	C(226)	0.712	0.067 2	0.684 5
P(1)	0.797(4)	0.169 2(1)	0.518 7(3)	C(221)	0.828	0.057 8	0.628 6
C(112)	0.711(1)	0.217 8(3)	0.380 8(9)	C(232)	1.138(1)	0.100 3(4)	0.605 4(7)
C(113)	0.631	0.227 8	0.302 1	C(233)	1.293	0.101 8	0.608 0
C(114)	0.538	0.201 1	0.259 2	C(234)	1.372	0.091 6	0.531 9
C(115)	0.525	0.164 5	0.295 1	C(235)	1.296	0.079 9	0.453 2
C(116)	0.605	0.154 5	0.373 8	C(236)	1.141	0.078 3	0.450 7
C(111)	0.698	0.181 2	0.416 6	C(231)	1.062	0.088 5	0.526 8

Table 4 Atomic coordinates for complex **8**

Atom	*x*	*y*	*z*	Atom	*x*	*y*	*z*
Bi	0.270 47(4)	0.342 31(5)	0.142 24(2)	C(116)	0.543 6(5)	0.674 7(8)	0.177 7(2)
Cl(1)	0.428 2(3)	0.237 6(8)	0.113 5(2)	C(111)	0.603 1	0.781 4	0.190 4
Cl(2)	0.219 8(3)	0.500 4(4)	0.203 6(1)	C(122)	0.626 2(4)	1.103 8(8)	0.166 8(3)
Mo(1)	0.200 10(7)	0.071 4(1)	0.167 68(3)	C(123)	0.631 8	1.248 3	0.171 8
C(11)	0.101 0(9)	0.208(2)	0.177 9(4)	C(124)	0.719 3	1.311 9	0.178 1
O(11)	0.040 3(7)	0.278(1)	0.187 7(3)	C(125)	0.801 2	1.231 1	0.179 3
C(12)	0.200(1)	0.057(1)	0.114 5(4)	C(126)	0.795 6	1.086 6	0.174 3
O(12)	0.197 7(8)	0.037(1)	0.084 5(3)	C(121)	0.708 1	1.023 0	0.168 1
C(13)	0.081(1)	−0.031(1)	0.157 6(4)	C(132)	0.847 6(7)	0.797(1)	0.213 1(2)
O(13)	0.011 2(7)	−0.087(1)	0.152 2(3)	C(133)	0.930 7	0.732 0	0.225 6
C(14)	0.352(1)	0.073(2)	0.195 5(4)	C(134)	0.970 6	0.625 5	0.205 5
C(15)	0.339(1)	−0.058(2)	0.180 2(6)	C(135)	0.927 4	0.583 5	0.173 0
C(16)	0.265(1)	−0.118(2)	0.197 5(6)	C(136)	0.844 3	0.647 9	0.160 5
C(17)	0.234(1)	−0.023(3)	0.224 2(5)	C(131)	0.804 4	0.754 4	0.180 6
C(18)	0.290(1)	0.090(2)	0.222 2(6)	P(2)	0.684 2(2)	0.762 1(3)	0.082 35(9)
Mo(2)	0.163 09(9)	0.472 5(1)	0.078 66(3)	C(212)	0.519 3(7)	0.909(1)	0.068 1(3)
C(21)	0.259(1)	0.354(2)	0.056 9(4)	C(213)	0.436 7	0.939 5	0.048 2
O(21)	0.312 1(9)	0.288(2)	0.041 4(4)	C(214)	0.412 0	0.860 9	0.017 7
C(22)	0.070(1)	0.345(2)	0.100 5(3)	C(215)	0.470 0	0.751 7	0.007 1
O(22)	0.009 4(8)	0.279(1)	0.108 7(3)	C(216)	0.552 7	0.721 1	0.027 0
C(23)	0.094(1)	0.394(2)	0.035 3(5)	C(211)	0.577 3	0.799 7	0.057 5
O(23)	0.053 0(8)	0.352(2)	0.011 5(3)	C(222)	0.646 3(5)	0.480 3(8)	0.084 7(2)
C(24)	0.253(2)	0.673(2)	0.095(1)	C(223)	0.665 2	0.338 4	0.080 0
C(25)	0.176(2)	0.667(2)	0.113 8(6)	C(224)	0.748 6	0.296 7	0.064 4
C(26)	0.095(2)	0.683(2)	0.095 0(9)	C(225)	0.813 0	0.397 0	0.053 6
C(27)	0.117(2)	0.695(2)	0.062 1(8)	C(226)	0.794 1	0.538 9	0.058 2
C(28)	0.205(2)	0.692(2)	0.059 6(8)	C(221)	0.710 7	0.580 6	0.073 8
N	0.672 7(8)	0.789(1)	0.123 5(3)	C(232)	0.768 2(5)	0.904(1)	0.026 0(2)
P(1)	0.698 4(2)	0.837 1(3)	0.162 74(8)	C(233)	0.838 8	0.984 5	0.011 2
C(112)	0.587 7(5)	0.844 4(8)	0.223 5(2)	C(234)	0.916 1	1.027 8	0.032 6
C(113)	0.512 8	0.800 7	0.243 9	C(235)	0.922 8	0.990 3	0.068 9
C(114)	0.453 3	0.694 0	0.231 3	C(236)	0.852 2	0.909 5	0.083 7
C(115)	0.468 7	0.631 0	0.198 2	C(231)	0.774 9	0.866 2	0.062 3

Table 5 Atomic coordinates for complex **9**·thf

Atom	*x*	*y*	*z*	Atom	*x*	*y*	*z*
Bi	0.073 25(3)	0.241 34(1)	0.083 19(2)	C(113)	0.555 7(5)	0.429 4(3)	0.0490(2)
Cl(1)	0.256 9(3)	0.180 6(1)	0.167 1(1)	C(114)	0.492 5	0.391 9	0.001 5
Cl(2)	−0.078 5(2)	0.353 1(1)	0.028 0(1)	C(115)	0.349 0	0.386 8	−0.009 8
Mo(1)	0.177 00(8)	0.167 14(4)	−0.015 20(4)	C(116)	0.268 6	0.419 2	0.026 2
C(11)	0.326(1)	0.220 3(5)	0.031 9(5)	C(111)	0.331 8	0.456 7	0.073 7
O(11)	0.421 9(8)	0.246 5(4)	0.056 9(4)	C(122)	0.248 6(6)	0.379 6(3)	0.184 2(2)
C(12)	0.272(1)	0.205 1(5)	−0.075 9(5)	C(123)	0.225 2	0.340 1	0.231 2
O(12)	0.329(1)	0.229 2(5)	−0.111 5(4)	C(124)	0.165 6	0.366 7	0.277 3
C(13)	0.029(1)	0.225 3(4)	−0.057 3(4)	C(125)	0.129 4	0.432 8	0.276 4
O(13)	−0.056 2(8)	0.251 9(4)	−0.087 4(3)	C(126)	0.152 8	0.472 3	0.229 3
C(14)	0.276(1)	0.063 8(5)	0.005 2(7)	C(121)	0.212 4	0.445 7	0.183 2
C(15)	0.213(1)	0.064 7(5)	−0.053 3(6)	C(132)	0.404 4(6)	0.568 5(2)	0.203 3(2)
C(16)	0.074(2)	0.069 9(5)	−0.055 5(6)	C(133)	0.481 4	0.623 7	0.223 2
C(17)	0.047(1)	0.077 3(5)	0.002 2(6)	C(134)	0.470 7	0.680 6	0.189 2
C(18)	0.173(2)	0.073 9(5)	0.040 8(5)	C(135)	0.382 8	0.682 3	0.135 3
Mo(2)	−0.181 74(8)	0.191 10(4)	0.123 36(4)	C(136)	0.305 7	0.627 1	0.115 3
C(21)	−0.058(1)	0.114 8(5)	0.139 4(5)	C(131)	0.316 5	0.570 2	0.149 3
O(21)	0.005 1(9)	0.067 7(4)	0.151 9(4)	C(141)	0.061 1(8)	0.515 2(4)	0.079 5(4)
C(22)	−0.230 4(9)	0.198 2(5)	0.035 4(5)	C(143)	−0.034 1(7)	0.603 9(3)	0.136 6(4)
O(22)	−0.271 6(9)	0.203 0(5)	−0.012 8(4)	C(144)	−0.115 0	0.624 3	0.178 2
C(23)	−0.308(1)	0.117 1(6)	0.104 2(6)	C(145)	−0.197 9	0.579 4	0.202 1
O(23)	−0.384(1)	0.073 8(5)	0.093 0(6)	C(146)	−0.200 0	0.514 0	0.184 6
C(24)	−0.296(1)	0.286 3(6)	0.146 9(5)	C(147)	−0.119 1	0.493 5	0.143 0
C(25)	−0.342(1)	0.233 9(6)	0.178 9(5)	C(142)	−0.036 2	0.538 4	0.119 0
C(26)	−0.227(1)	0.211 3(6)	0.218 7(5)	O(9)	0.426(2)	0.945 2(8)	0.221 5(8)
C(27)	−0.110(1)	0.248 5(5)	0.210 4(5)	C(91)	0.406(4)	0.967(1)	0.163(1)
C(28)	−0.153(1)	0.294 9(5)	0.166 9(5)	C(92)	0.304(4)	0.927(1)	0.130(1)
P	0.231 3(2)	0.496 7(1)	0.121 6(1)	C(93)	0.296(4)	0.867(1)	0.171(1)
C(112)	0.475 3(5)	0.461 8(3)	0.085 0(2)	C(94)	0.382(3)	0.877 2(9)	0.219 6(8)

Table 6 Atomic coordinates for complex **13**

Atom	*x*	*y*	*z*	Atom	*x*	*y*	*z*
Bi	0.227 90(4)	0.158 26(6)	0.357 84(2)	C(116)	0.269 1(7)	0.099 1(1)	0.026 0(2)
Cl(1)	0.072 1(4)	0.270 8(8)	0.387 3(2)	C(111)	0.275 4	0.134 9	0.062 5
Cl(2)	0.279 2(3)	−0.000 9(4)	0.295 5(1)	C(122)	0.015 6(8)	0.094(1)	0.066 7(3)
W(1)	0.337 44(5)	0.026 84(6)	0.421 20(2)	C(123)	−0.066 3	0.061 8	0.046 0
C(11)	0.429(1)	0.155(2)	0.400 3(5)	C(124)	−0.089 9	0.140 0	0.015 1
O(11)	0.491 3(9)	0.223(1)	0.389 9(4)	C(125)	−0.031 7	0.250 2	0.004 8
C(12)	0.240(1)	0.148(2)	0.442 9(4)	C(126)	0.050 2	0.282 2	0.025 4
O(12)	0.186(1)	0.209(2)	0.459 4(4)	C(121)	0.073 9	0.204 0	0.056 4
C(13)	0.408(1)	0.103(2)	0.464 0(6)	C(132)	0.294 6(6)	0.462 3(9)	0.058 3(3)
O(13)	0.448(1)	0.149(2)	0.489 4(4)	C(133)	0.314 9	0.604 9	0.054 5
C(14)	0.403(2)	−0.189(3)	0.406 1(7)	C(134)	0.250 8	0.705 8	0.065 7
C(15)	0.382(3)	−0.197(2)	0.438 4(8)	C(135)	0.166 3	0.664 1	0.080 8
C(16)	0.291(2)	−0.195(2)	0.440 9(8)	C(136)	0.146 0	0.521 5	0.084 6
C(17)	0.252(2)	−0.175(2)	0.407(1)	C(131)	0.210 1	0.420 6	0.073 4
C(18)	0.325(4)	−0.167(2)	0.384 0(7)	P(2)	0.197 1(3)	0.163 5(4)	0.162 9(1)
W(2)	0.299 72(4)	0.428 83(6)	0.331 84(2)	C(212)	0.125 8(5)	−0.104 1(9)	0.166 8(3)
C(21)	0.399(1)	0.291(2)	0.320 9(4)	C(213)	0.130 3	−0.249 5	0.171 3
O(21)	0.459 2(8)	0.218(1)	0.313 3(3)	C(214)	0.217 7	−0.315 1	0.177 5
C(22)	0.420(1)	0.529(2)	0.342 5(4)	C(215)	0.300 6	−0.235 4	0.179 1
O(22)	0.490 7(8)	0.588(1)	0.347 8(4)	C(216)	0.296 1	−0.089 9	0.174 6
C(23)	0.296(1)	0.445(2)	0.385 9(6)	C(211)	0.208 7	−0.024 3	0.168 4
O(23)	0.300(1)	0.464(1)	0.415 8(4)	C(222)	0.087 1(6)	0.152 7(9)	0.223 3(2)
C(24)	0.266(1)	0.531(2)	0.276 2(6)	C(223)	0.012 4	0.195 3	0.244 3
C(25)	0.210(1)	0.412(2)	0.277 9(6)	C(224)	−0.047 7	0.303 3	0.232 2
C(26)	0.147(1)	0.427(2)	0.304 5(5)	C(225)	−0.033 0	0.368 6	0.199 1
C(27)	0.162(2)	0.558(3)	0.319 9(6)	C(226)	0.041 8	0.325 9	0.178 2
C(28)	0.233(2)	0.619(2)	0.300 5(7)	C(221)	0.101 8	0.217 9	0.190 3
N	0.169 0(9)	0.210(1)	0.122 7(3)	C(232)	0.347 8(7)	0.206(1)	0.212 8(2)
P(1)	0.182 9(3)	0.239 1(4)	0.082 0(1)	C(233)	0.431 3	0.270 8	0.225 3
C(112)	0.352 5(7)	0.089(1)	0.084 2(2)	C(234)	0.471 1	0.377 7	0.205 0
C(113)	0.423 2	0.007 9	0.069 3	C(235)	0.427 5	0.419 3	0.172 3
C(114)	0.416 9	−0.027 9	0.032 7	C(236)	0.344 1	0.354 0	0.159 8
C(115)	0.339 8	0.017 7	0.011 1	C(231)	0.304 2	0.2472	0.180 0

Table 7 Crystallographic data *

Compound	**2**	**8**	**9**·thf	**13**
Formula	$C_{50}H_{40}BiCl_2Fe_2NO_4P_2$	$C_{52}H_{40}BiCl_2Mo_2NO_6P_2$	$C_{41}H_{32}BiCl_2Mo_2O_6P{\cdot}C_4H_8O$	$C_{52}H_{40}BiCl_2NO_6P_2W_2$
M	1172.4	1308.6	1195.6	1484.4
Space group	$P2_1/n$	$P2_1/c$	$P2_1/c$	$P2_1/c$
a/Å	9.009(2)	14.197(2)	9.807(3)	14.129(3)
b/Å	35.049(9)	9.556(2)	20.425(5)	9.513(2)
c/Å	14.796(5)	37.190(7)	22.945(7)	37.020(8)
β/°	91.81(3)	92.12(2)	98.88(4)	92.26(2)
U/Å^3	4669.6	5042.1	4541.0	4972.2
D_c/g cm^{-3}	1.667	1.724	1.748	1.983
μ/mm^{-1}	4.59	4.17	4.59	8.46
$F(000)$	2312	2552	2328	2808
Crystal size/mm	0.15 × 0.31 × 0.38	0.08 × 0.35 × 0.38	0.19 × 0.23 × 0.42	0.27 × 0.29 × 0.38
Transmission factors	0.116–0.225	0.175–0.270	0.127–0.231	0.027–0.063
$2\theta_{max}$/°	45	50	50	50
Reflections measured	9700	9903	8311	9407
Unique reflections	6101	8875	7980	8735
Observed reflections, N	3564	4758	5210	5968
R_{int}	0.0362	0.0778	0.0592	0.0597
No. of refined parameters, P	487	520	475	523
R	0.0742	0.0583	0.0454	0.0549
$R' = (\Sigma w\Delta^2/\Sigma wF_o^2)^{\frac{1}{2}}$	0.0633	0.0557	0.0483	0.0684
Goodness of fit = $[\Sigma w\Delta^2/(N-P)]^{\frac{1}{2}}$	1.05	1.06	1.09	1.00
Mean, maximum shift/e.s.d.	0.003, 0.009	0.004, 0.014	0.031, 0.170	0.002, 0.008
Maximum, minimum electron density/e Å^{-3}	2.83, −1.11	2.08, −0.90	1.67, −1.63	4.25, −2.11

* Details in common: monoclinic, $Z = 4$.

A **B** **C** **D**

the bond distances to the axial and equatorial groups have been discussed by Aurivillius and Malmros[19] although we will not comment further on this matter at this time. Another highly symmetrical geometry for AB_4E is the apically vacant, square-based pyramid, **B**.[13] This is not a common co-ordination type but is found in the structure of tin and lead monoxide, SnO and PbO.[20a],†

The structures of **2** and **9** fall within a third class illustrated in **C**, the major difference between this and **A** being that the axial groups bend away from the equatorial groups. Another example of this structure type is the tellurium complex $[TeCl_2(NPPh_3)_2]$ for which the inter-axial, Cl–Te–Cl angle is 162.7°[21] together with the bismuth complex $[PPh_4][BiBr_2Ph_2]$ (α = 95.9, β = 177.3°).[22] A final structure type is the tetrahedron, **D**, although for an AB_4E compound, this requires that the lone pair is considered stereochemically inactive. We are aware of only one example of a tetrahedral complex with ten valence electrons at the central atom, namely the anion $[Bi\{Co(CO)_4\}_4]^-$ **18**. Complex **18** was structurally characterised as its $[Co(\eta\text{-}C_5H_5)_2]^+$ salt by Leigh and Whitmire[23] and has a symmetry close to T_d. These authors comment on the stereochemical inactivity of the lone pair and also on the exceptionally long Bi–Co bond lengths and the fact that the cluster is paramagnetic. The structure of **18** as its $[NMe_4]^+$ salt has also been reported by Martinengo *et al.*[24] and similar comments were made, although in this case, a slight distortion towards C_{2v} symmetry is evident in the Co–Bi–Co angles and no mention is made of any paramagnetism. The structures of **8** and **13** are clearly geometrically intermediate between types **C** and **D**.

† *Note added at proof.* A recent structure determination of $BiMg_2VO_6$ reveals a four-co-ordinate bismuth(III) centre in which the bismuth is bonded to four oxygens with a rectangular pyramidal geometry similar to **B**.[20b]

Electronic Structure.—We now turn to a discussion of possible electronic factors which might influence the structure adopted by AB_4E type molecules. In the structures we report in this paper there is a notable deformation from the archetypal geometry expected from VSEPR (disphenoidal with β ≈ 180°) to one in which the Cl–Bi–Cl angle is substantially non-linear, being reduced by between 25 and 42° towards a quasi-tetrahedral geometry at bismuth. Such a distortion may well derive from the bulkiness of the metal-based substituents attached to the bismuth but this is unlikely to be a dominant factor in view of the relatively small values for the angle α, especially for **2**. Alternative explanations based on electronic factors can also be advanced and among the possibilities to be considered are the following: (1) the electronegativity (or rather the lack of it!) of the metal substituents as compared with, for example, species with halide or oxygen ligands in the equatorial sites of ten-electron AB_4E species; (2) the possibility of π donation (in addition to the σ interactions) from the metal ligands to the $BiCl_2$ unit; (3) the different overlap characteristics of metal ligands compared with p-block elements. To explore these ideas fully and to examine their relationship with those governing geometric distortions in systems with two fewer valence electrons, where distortions from VSEPR-predicted structures also occur, is beyond the scope of this paper and will form a future publication.[25] In this paper we will confine ourselves to considering the basic features of the electronic structure of compounds such as **8**, emphasising their relationship to other ten-electron four-co-ordinate main group species, and the extent of π bonding in these complexes.[7]

As an initial probe of the electronic structures of ten-electron AX_2M_2E complexes of the type seen in compounds **2**–**4**, **8**–**11**, **13** and **14** we have carried out extended Hückel molecular-orbital (EHMO) calculations[26a,b] on the model complex $[SbCl_2\{Mo(CO)_3(\eta\text{-}C_5H_5)\}_2]^-$ **E** at a variety of geometries in which interbond angles and torsion angles about bonds were varied, but with bond distances held at idealised but realistic values (based on the crystal structures). In addition, fragment molecular-orbital analysis was carried out on the construction of the final MOs from the orbitals of the $[SbCl_2]^+$ and $[\{Mo(CO)_3(\eta\text{-}C_5H_5)\}_2]^{2-}$ units. Use of published parameters

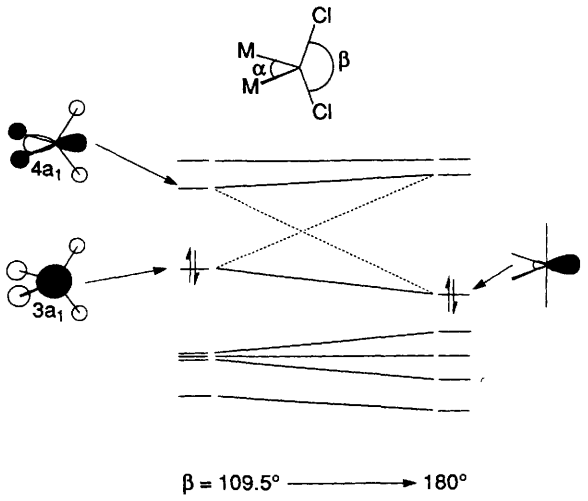

Fig. 6 Partial orbital correlation diagram[27] for the tetrahedron-to-butterfly distortion of a $SbCl_2M_2$ fragment [M = 17e-metal ligand, *e.g.* $\{Mo(CO)_3(\eta\text{-}C_5H_5)\}$ or $\{Fe(CO)_2(\eta\text{-}C_5H_5)\}$]

for bismuth[26c] for the bismuth analogue of **E**, *i.e.* **8**/**9**, led to unrealistic electronic structures (*i.e.* with very small HOMO–LUMO gaps, hence probably high spin) leading us to doubt the generality of these parameters. In contrast use of published parameters for antimony[26d] (or indeed with a second set of published parameters for bismuth[26e] which gives results very similar to those for **E**) led to much more chemically sensible electronic structures as summarised below. We will return to a full comparison of the behaviour of bismuth and antimony in these species and simpler analogues, and the appropriate parameterisation for bismuth (and the related problem of how relativistic effects for this element should be accounted for in EHMO calculations) in the future.[25]

As noted above the archetypal geometry for AB_4E systems with ten valence electrons around the central p-block element, A, is disphenoidal. An excellent summary of the reasons for this preference using the language of qualitative molecular-orbital theory has been provided by Gimarc.[27] Furthermore, this analysis rationalised the preference for electronegative substituents in asymmetric species to occupy the axial sites (*e.g.* in species of the general form AX_2Y_2E). This analysis forms the basis for our discussion of the structures reported in this paper and we will therefore summarise the pertinent details (see Fig. 6). The distortion of the angles at the ten-electron central atom, A, away from tetrahedral values is driven by stabilisation of the lone pair (orbital $3a_1$ in Gimarc's nomenclature) which is the HOMO of the AB_4E species. This distortion is driven by two factors. The first is enhanced (bonding) overlap between the substituent atoms, **B**, as B–A–B angles decrease (four go from 109.5 to 90°, and one, α in Fig. 6, remains at 109.5° and only one, β, increases from 109.5 to 180°). The second factor is mixing between $4a_1$ and $3a_1$ which is possible in the reduced symmetry (C_{2v}) of the disphenoidal species but not for a regular tetrahedron (T_d symmetry). This mixing causes the lone pair ($3a_1$) to develop atom A p character and become hybridised in the classic lone pair manner. This mixing is most pronounced when the central atom is electropositive and hence $4a_1$ relatively low in energy as is the case when A = Bi or Sb. Further subtleties discussed by Gimarc include the tendency of the axial ligands in these species to bend *away* from the lone pair (*i.e.* β > 180°), in order to reduce antibonding interactions between the B atom orbitals and the A atom lone pair in $3a_1$, and the tendency of electronegative equatorial substituents to favour smaller values of α (*i.e.* α < 109.5°).

Our calculations on species **E** confirm that it conforms to Gimarc's general conclusions and provide details relevant to the asymmetric AX_2M_2E system [in **E**, A = Sb, X = Cl, M = $\{Mo(CO)_3(\eta\text{-}C_5H_5)\}$]. Figs. 6 and 7 illustrate in schematic form the outcome of these calculations. The key features are: (1) that the HOMO of **E** is the hybridised Sb lone pair, whose energy rises as β decreases from 180° towards 109.5°; (2) the LUMO of the $[SbCl_2]^+$ fragment is the $SbCl_2$ σ* orbital ($2b_1$), whose energy falls as β decreases; (3) the preferred (*i.e.* lowest calculated energy) geometry has the Cl–Sb–Cl angle β *ca.* 165° and the Mo–Sb–Mo angle α *ca.* 120° as judged by two-dimensional searches of the (α, β) space. These results are in accord with the observed structures and with the Gimarc analysis, the latter with various caveats. First the lowered symmetry here present (at most C_{2v} even when α = β = 109.5°) allows orbital mixings of the type discussed above for the AB_4E system at all geometries. Secondly, the distortion of β is in the opposite sense to that observed, for example, in SF_4 (in which β = 187°). This might be ascribed to the orbital characteristics of $3a_1$ which is much more centred on antimony in **E** than for the archetypal AB_4E species (because the axial substituents are so electronegative relative to the central atom) thereby removing part of the driving force for contraction of B···B (or X···Y) distances.

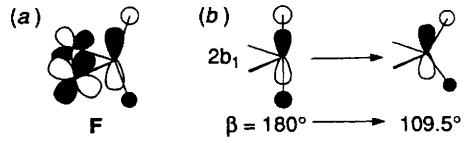

Fig. 7 (*a*) Illustration of the π interaction, **F**, between the metal ligands and the $BiCl_2$ unit in $BiCl_2M_2$ fragments [M = 17e-metal ligand, *e.g.* $\{Mo(CO)_3(\eta\text{-}C_5H_5)\}$ or $\{Fe(CO)_2(\eta\text{-}C_5H_5)\}$]. (*b*) Variation in $SbCl_2^+$ fragment LUMO ($2b_1$) with change in β

In contrast to the Gimarc analysis[27] which focuses exclusively on σ-bonding effects, our calculations allow for the possibility of π interactions between the metal-based M ligands and the Sb centre. In principle the $2b_1$ orbital may act as a π-acceptor functionality on the $SbCl_2$ fragment. This type of π acceptor (*i.e.* through inverse- or negative-hyperconjugation) has attracted considerable recent attention (see *e.g.* refs. 28 and 29). The amount of π donation from the equatorial metal ligands was investigated by fragment molecular-orbital analysis. Fragment orbital populations were determined for fragments $[SbCl_2]^+$ and $[\{Mo(CO)_3(\eta\text{-}C_5H_5)\}_2]^{2-}$ for **E** at a range of geometries from β = 135 to 175° in order to observe the occupancy of the Cl–Sb–Cl σ* orbital ($2b_1$). The π interaction between this orbital and the Mo d_π orbitals (see **F**, Fig. 7), increases in strength (as measured by occupancy of the $2b_1$ LUMO in the $SbCl_2$ fragment) as the angle β decreases from 180°. Thus the occupancy of $2b_1$ rises from 0.075 at β = 175° to 0.126 at β = 135° and the MO resulting (**F**) falls smoothly in energy as β decreases. The observed values for β therefore result, at least in part, from a balance between the destabilisation of the HOMO and the stabilisation of orbital **F** as β decreases from 180 towards 109.5°.

The π-donating ability of ML_n fragments and the preferred orientation of π acceptors attached to them has been discussed by Hoffmann and co-workers [see, *e.g.* ref. 30 for the case of $(C_5H_5)ML_3$ species such as are present in **E** fragments]. Their conclusion was that there is a (weak) preference for the π-acceptor orbital to be aligned parallel to the plane of the cyclopentadienyl ligand in the $(C_5H_5)ML_3$ [or $(C_5H_5)ML_2$] unit. For **E** the $2b_1$ orbital is the π-acceptor orbital and its misorientation relative to the plane of the C_5H_5 ligand in the observed structures of **2**, **8**, **9** and **13** can be monitored by noting the inclination of the $BiCl_2$ unit relative to the Bi–M–(C_5H_5) centroid planes (which are 15.7 and 79.9° for **2**, 12.4 and 29.4° for **8**, 32.9 and 0.2° for **9**, 27.7 and 13.3° for **13**). Therefore all the metal fragments [except for one $Fe(CO)_2(\eta\text{-}C_5H_5)$ unit] lie close (<35°) to the orientation in which the metal-to-bismuth π donation would be at a maximum.

The change in total energy as Cl–M–Cl angle β was varied (with α = 118°) was calculated thus giving a measure of the softness of the axial angle. The variability of Cl–Bi–Cl angle with counter ion for **8** and **9** is particularly notable and itself an indication that this angle is soft. In accord with this observation we find variations of *ca.* 2 kJ mol^{-1} per degree change in β in the total energy near the observed values for **8** and **9**.

In summary therefore, on the basis of the structural data to hand and these initial EHMO studies, we conclude that the presence of π-donating substituents Y in the pseudo-equatorial sites of an AX_2Y_2E species may promote a distortion of the sort where β decreases from 180° as depicted in Figs. 6 and 7 for **E**, and observed in **2**, **8**, **9** and **13**. This type of distortion will be most pronounced when the AX_2 fragment $2b_1$ σ* orbital is low in energy and centred on the A atom, *i.e.* when A is relatively electropositive and X relatively electronegative. With this in mind, it is instructive to look for other examples in the literature to test the generality of these ideas. We have already mentioned the tellurium complex, $[TeCl_2(NPPh_3)_2]$, described by Roesky *et al.*[21] and a recent example from xenon chemistry, reported by Turowsky and Seppelt,[31] is also relevant, namely $[XeO_2(OTeF_5)_2]$. Both complexes adopt a structure of type **C** (explicitly commented upon by the authors), with β = 162.7 and 163.7° respectively, and have potentially strong π-donor ligands in the pseudo-equatorial sites, $NPPh_3$ and O respectively, which could account for the unusual structures. Moreover, these arguments should be more generally applicable to compounds with different co-ordination numbers and in this regard we note the structures of two other molecules. In the stucture of $[MoO_2F_2(bipy)]$[32] (bipy = 2,2′-bipyridine), the *trans* fluorine ligands have an interbond angle of 154.4° such that they are bent *away* from the *cis* π-donor oxygen atoms towards the *larger* bipy ligand. Also, in $XeOF_4$,[13] the O–Xe–F angle is 91.6(2)°, *i.e.* the fluorines are tipped *towards* the lone pair. VSEPR theory usually assumes that lone-pair repulsions are greater than double-bond repulsions and as such, this structure is at odds (albeit only slightly) with this prediction. Both of these distortions are consistent with the bonding model discussed above.

As we have mentioned, these ideas can be described as examples of the structural consequences of inverse- or negative-hyperconjugation, a subject which has received significant recent attention especially from Reed and Schleyer.[28] In the particular examples described in this paper, the important effect of π bonding on the stereochemical activity of a lone pair has been addressed. It can be seen that strong π bonding of this sort may exert a significant influence on the co-ordination geometry and therefore that traditional ideas based on the stereochemical influence of a lone pair(s), or lack of it, may sometimes be inadequate in understanding certain structures.

Experimental

General Considerations.—All experiments were performed under an atmosphere of dry, oxygen-free dinitrogen using standard Schlenk techniques. All solvents were dried and distilled over appropriate drying agents immediately prior to use. Infrared spectra were recorded on a Nicolet 20 SXB FTIR spectrophotometer and microanalytical data were obtained at the University of Newcastle. Proton and ^{13}C NMR spectra were obtained on a Bruker WP 200 spectrometer operating at 200.13 and 50.324 MHz respectively and referenced to $SiMe_4$. All reagents were procured commercially, and used without further purification, or prepared by literature methods referenced where appropriate.

Analytical and infrared data for all new complexes are given in Table 1.

Preparations.—$[N(PPh_3)_2][BiCl_2\{Fe(CO)_2(\eta\text{-}C_5H_5)\}_2]$ **2**. A sample of $[N(PPh_3)_2]Cl$ (0.078 g, 0.135 mmol) was added to a dark green solution of **1**[1,8] (0.081 g, 0.135 mmol) dissolved in thf (20 cm^3) and the mixture stirred overnight. This resulted in no visible colour change. The solution was filtered through Celite and the solvent removed by vacuum affording a dark green solid which was redissolved in thf (5 cm^3). Hexane (30 cm^3) was layered over this solution and solvent diffusion over a period of days at −25 °C afforded **2** as a dark green crystalline powder (0.144 g, 91%). Crystals suitable for X-ray diffraction were obtained after a second recrystallisation from thf–Et_2O (5–20 cm^{-3}). NMR (CD_2Cl_2): ^1H, δ 4.96 (s, 10 H, C_5H_5) and 7.4–7.6 [m, 30 H, $N(PPh_3)_2$]; $^{13}C\text{-}\{^1H\}$, δ 85.4 (s, C_5H_5), 134.1, 132.5 and 129.9 [m, *o*-, *m*-, *p*-phenyls, $N(PPh_3)_2$].

The $[NMe_4]^+$ salt $[NMe_4][BiCl_2\{Fe(CO)_2(\eta\text{-}C_5H_5)\}_2]$ **3** was prepared in a similar manner as was the bromide derivative **4** from the starting complex **5**.[8]

$[BiI\{Fe(CO)_2(\eta\text{-}C_5H_5)\}_2]$ **6**. Samples of $[Bi\{Fe(CO)_2(\eta\text{-}C_5H_5)\}_3]$[1,8] (0.406 g, 0.549 mmol) and I_2 (0.139 g, 0.549 mmol) were dissolved in thf (20 cm^3) and produced a green–brown solution which was stirred for 20 min. After this time the solution was filtered through Celite and the solvent removed by vacuum leaving a green–brown solid. This solid was washed with hexane (4 × 10 cm^3) to remove most of the $[FeI(CO)_2(\eta\text{-}C_5H_5)]$ which is also produced in the reaction. The remaining solid was dissolved in thf (5 cm^3) and hexane (30 cm^3) was layered over this. Solvent diffusion over a period of days at −30 °C afforded **6** as a green–brown powder (0.10 g, 25%). Compound **6** is not very stable in solution and readily decomposes to give $[FeI(CO)_2(\eta\text{-}C_5H_5)]$.

$[N(PPh_3)_2][BiCl_2\{Mo(CO)_3(\eta\text{-}C_5H_5)\}_2]$ **8**. To a suspension of $[N(PPh_3)_2]Cl$ (0.249 g, 0.434 mmol) in thf (10 cm^3), 1 equivalent of **7**[2] (0.319 g, 0.434 mmol) in thf (10 cm^3) was added. The mixture was stirred for 16 h during which time the initial dark green colour remained unchanged. After this time, the solution was filtered through Celite and all solvent was removed by vacuum. The resulting dark green solid was redissolved in thf (5 cm^3) and hexane (30 cm^3) was layered over this. Solvent diffusion over a period of days at −22 °C afforded **8** as a dark green powder (0.54 g, 95%). Crystals suitable for X-ray diffraction were obtained by recrystallisation from CH_2Cl_2–Et_2O mixtures by solvent diffusion. ^1H NMR (CD_2Cl_2): δ 5.49 (s, 10 H, C_5H_5) and 7.4–7.7 [m, 30 H, $N(PPh_3)_2$].

Complex **9** was prepared in an analogous manner using $[PPh_3(CH_2Ph)]Cl$ and in similar yields. Crystals suitable for X-ray diffraction were obtained by solvent diffusion of a 1:1 mixture of thf–hexane (40 cm^3) into a solution of **9** in CH_2Cl_2 (6–7 cm^3). ^1H NMR (CD_2Cl_2): δ 4.90 (d, 2 H, $^2J_{PH}$ 15.3 Hz, CH_2Ph), 5.46 (s, 10 H, C_5H_5) and 7.2–7.8 (m, 20 H, PPh_3CH_2Ph).

The bromide complexes **10** and **11** were also prepared similarly from **12**[5] and $[PPh_4]Br$ and $[NBu^n_4]Br$ respectively in good yield. ^1H NMR for **10** (CD_2Cl_2): δ 5.51 (s, 10 H, C_5H_5) and 7.5–7.9 (m, 20 H, PPh_4).

The tungsten complexes **13** and **14** were prepared from **15**[2] and 1 equivalent of $[N(PPh_3)_2]Cl$ and $[PPh_3(CH_2Ph)]Cl$ respectively and also in good yields. ^1H NMR for **13** (CD_2Cl_2): δ 5.62 (s, 10 H, C_5H_5) and 7.4–7.7 [m, 30 H, $N(PPh_3)_2$].

$[N(PPh_3)_2][BiCl_3\{Mo(CO)_3(\eta\text{-}C_5H_5)\}]$ **16**. *Method A.* Compound **8** (0.140 g, 0.107 mmol) and $[N(PPh_3)_2][BiCl_4]$ (0.095 g, 0.107 mmol) were added to a flask and dissolved in CH_2Cl_2 (10 cm^3) giving a red-orange solution. This was stirred for 3 d, during which time no colour change took place, and then Et_2O (20 cm^3) was layered over the solution. Cooling to −30 °C for a period of days afforded copper-coloured flakes of **16**.

Method B. The salt $[N(PPh_3)_2]Cl$ (0.127 g, 0.221 mmol) was dissolved in thf (10 cm^3) and this was added to a solution of $[BiCl_2\{Mo(CO)_3(\eta\text{-}C_5H_5)\}]$ (0.116 g, 0.221 mmol) (prepared as in ref. 2) in thf (10 cm^3). This resulted in a yellow–green solution which became green–brown upon complete addition. The resulting mixture was stirred for 18 h and then filtered through Celite. After removal of all solvent by vacuum, a

yellow–green solid remained which was redissolved in thf (15 cm^3) and layered with Et_2O (35 cm^3). Solvent diffusion over a period of days at −30 °C gave a dark green solid which was recrystallised from CH_2Cl_2–Et_2O to give copper-coloured **16**.

X-Ray Crystallography.—Crystals of compounds **2**, **8**, **9**·thf and **13**, sealed in Lindemann glass capillaries, were examined on a Stoe-Siemens diffractometer with graphite-monochromated radiation (λ = 0.710 73 Å), at room temperature (**2** and **8**) or 240 K (**9**·thf and **13**).[33] Crystal data are listed in Table 7, together with other information on the structure determinations. Cell parameters were refined from 2θ values (20–25°) of 32 reflections measured at ±ω in each case. Intensities were measured with ω–θ scans and on-line profile fitting.[34] Semi-empirical absorption corrections were applied,[35] together with small decay corrections for **2** and **8**, based on periodic measurement of three standard reflections. Each data set consisted of a complete unique set of reflections, together with a partial set of equivalent reflections. Unique reflections with $F > 4\sigma(F)$ were used in structure determination.

Atoms were located from Patterson and difference syntheses and refined[35] with anisotropic thermal parameters by blocked-cascade methods to minimise $\Sigma w\Delta^2$, with $\Delta = |F_o| - |F_c|$ and $w = 1/\sigma^2(F)$; $\sigma^2(F)$ included contributions from the counting statistics and from an empirical analysis of the variance of observed and calculated data.[36] Isotropic H atoms were constrained to give C–H 0.96 Å on the angle external bisectors of the rigid group ideal hexagon phenyl rings (with C–C 1.395 Å), $U(H) = 1.2U_{eq}(C)$. Extinction effects were negligible. Atomic scattering factors were taken from ref. 37. The largest peaks in the final difference syntheses were close to the heavy atoms.

Additional material available from the Cambridge Crystallographic Data Centre comprises H-atom coordinates, thermal parameters and remaining bond lengths and angles.

Acknowledgements

We thank the SERC for support and BP Research (Sunbury) for CASE Awards to N. A. C. and G. A. F.; N. C. N. also thanks the Royal Society for additional supporting funds.

References

1 W. Clegg, N. A. Compton, R. J. Errington and N. C. Norman, *J. Chem. Soc., Dalton Trans.*, 1988, 1671.
2 W. Clegg, N. A. Compton, R. J. Errington, N. C. Norman, A. J. Tucker and M. J. Winter, *J. Chem. Soc., Dalton Trans.*, 1988, 2941.
3 W. Clegg, N. A. Compton, R. J. Errington, D. C. R. Hockless, N. C. Norman, M. Ramshaw and P. M. Webster, *J. Chem. Soc., Dalton Trans.*, 1990, 2375.
4 N. A. Compton, R. J. Errington, G. A. Fisher, N. C. Norman, P. M. Webster, P. S. Jarrett, S. J. Nichols, A. G. Orpen, S. E. Stratford and N. A. L. Williams, *J. Chem. Soc., Dalton Trans.*, 1991, 669.
5 W. Clegg, N. A. Compton, R. J. Errington, G. A. Fisher, D. C. R. Hockless, N. C. Norman, N. A. L. Williams, S. E. Stratford, S. J. Nichols, P. S. Jarrett and A. G. Orpen, *J. Chem. Soc., Dalton Trans.*, 1992, 193.
6 N. C. Norman, *Chem. Soc. Rev.*, 1988, **17**, 269.
7 W. Clegg, N. A. Compton, R. J. Errington, G. A. Fisher, D. C. R. Hockless, N. C. Norman and A. G. Orpen, *Polyhedron*, 1991, **10**, 123.
8 J. M. Wallis, G. Müller and H. Schmidbaur, *J. Organomet. Chem.*, 1987, **325**, 159.
9 L. M. Clarkson, W. Clegg, N. C. Norman, A. J. Tucker and P. M. Webster, *Inorg. Chem.*, 1988, **27**, 2653.
10 L. M. Clarkson, W. Clegg, D. C. R. Hockless, N. C. Norman and T. B. Marder, *J. Chem. Soc., Dalton Trans.*, 1991, 2229.
11 L. M. Clarkson, W. Clegg, D. C. R. Hockless, N. C. Norman, L. J. Farrugia, S. G. Bott and J. L. Atwood, *J. Chem. Soc., Dalton Trans.*, 1991, 2241.
12 J. M. Wallis, G. Müller, J. Riede and H. Schmidbaur, *J. Organomet. Chem.*, 1989, **369**, 165.
13 R. J. Gillespie and I. Hargittai, *The VSEPR Model of Molecular Geometry*, Allyn and Bacon, Boston, 1991.
14 J. E. Huheey, *Inorganic Chemistry*, 2nd edn., Harper and Row, New York, 1978, pp. 145–147.
15 Z. Galdecki, M. L. Glowka and B. Golinski, *Acta Crystallogr., Sect. B*, 1976, **32**, 2319.
16 D. H. R. Barton, B. Charpiot, E. Tran Huu Dau, W. B. Motherwell, C. Pascard and C. Pichon, *Helv. Chim. Acta*, 1984, **67**, 586.
17 S. K. Blower and C. Greaves, *Acta Crystallogr., Sect. C*, 1988, **44**, 587.
18 P. Lightfoot, J. A. Hriljac, S. Pei, Y. Zheng, A. W. Mitchell, D. R. Richards, B. Dabrowski, J. D. Jorgensen and D. G. Hinks, *J. Solid State Chem.*, 1991, **92**, 473.
19 B. Aurivillius and G. Malmros, *K. Tekn. Hogsk. Handl.*, 1972, **291**, 544.
20 (*a*) A. F. Wells, *Structural Inorganic Chemistry*, Clarendon Press, Oxford, 1984, pp. 557–558; (*b*) J. Huang and A. W. Sleight, *J. Solid State Chem.*, 1992, **100**, 170.
21 H. W. Roesky, J. Münzenberg, R. Bohra and M. Noltemeyer, *J. Organomet. Chem.*, 1991, **418**, 339; M. Björgvinsson and H. W. Roesky, *Polyhedron*, 1991, **10**, 2353.
22 W. Clegg, R. J. Errington, G. A. Fisher, D. C. R. Hockless, N. C. Norman, A. G. Orpen and S. E. Stratford, *J. Chem. Soc., Dalton Trans.*, 1992, 1967.
23 J. S. Leigh and K. H. Whitmire, *Angew. Chem., Int. Ed. Engl.*, 1988, **27**, 396.
24 S. Martinengo, A. Fumagalli, G. Ciani and M. Moret, *J. Organomet. Chem.*, 1988, **347**, 413.
25 N. C. Norman, A. G. Orpen, C. Mealli and S. E. Stratford, unpublished work.
26 (*a*) J. Howell, A. Rossi, D. Wallace, I. K. Harak and R. Hoffmann, *Quantum Chemistry Program Exchange*, 1977, **10**, 344; (*b*) C. Mealli and D. M. Proserpio, *J. Chem. Educ.*, 1990, **67**, 399; (*c*) L. L. Lohr, jun., and P. Pykko, *Chem. Phys. Lett.*, 1979, **62**, 333; (*d*) T. Hughbanks, R. Hoffmann, M.-H. Whangbo, K. R. Stewart, O. Eisenstein and E. Canadell, *J. Am. Chem. Soc.*, 1982, **104**, 3876; (*e*) K. H. Whitmire, T. A. Albright, S.-K. Kang, M. R. Churchill and J. C. Fettinger, *Inorg. Chem.*, 1986, **25**, 2799.
27 B. M. Gimarc, *Molecular Structure and Bonding*, Academic Press, New York, 1979, p. 64ff; B. M. Gimarc and S. A. Khan, *J. Am. Chem. Soc.*, 1978, **100**, 2340.
28 A. E. Reed and P. von R. Schleyer, *J. Am. Chem. Soc.*, 1990, **112**, 1434.
29 A. G. Orpen and N. G. Connelly, *Organometallics*, 1990, **9**, 1206.
30 P. Kubacek, R. Hoffmann and Z. Havlas, *Organometallics*, 1982, **1**, 180.
31 L. Turowsky and K. Seppelt, *Z. Anorg. Allg. Chem.*, 1992, **609**, 153.
32 I. Sens, H. Stenger, U. Müller and K. Dehnicke, *Z. Anorg. Allg. Chem.*, 1992, **610**, 117.
33 J. Cosier and A. M. Glazer, *J. Appl. Crystallogr.*, 1986, **19**, 105.
34 W. Clegg, *Acta Crystallogr., Sect. A*, 1981, **37**, 22.
35 G. M. Sheldrick, SHELXTL, an integrated system for solving, refining and displaying crystal structures from diffraction data, revision 5, University of Göttingen, 1985; SHELXS 86, program for crystal structure determination, 1986.
36 Wang Hong and B. E. Robertson, *Structure and Statistics in Crystallography*, ed. A. J. C. Wilson, Adenine Press, New York, 1985, p. 125.
37 *International Tables for X-Ray Crystallography*, Kynoch Press, Birmingham, 1974, vol. 4, pp. 99, 149.

Received 7*th July* 1992; *Paper* 2/03575H